

Global and regional trends in mercury emissions and concentrations, 2010–2015[☆]



David G. Streets^{a,*}, Hannah M. Horowitz^b, Zifeng Lu^a, Leonard Levin^c, Colin P. Thackray^d, Elsie M. Sunderland^{d,e}

^a Energy Systems Division, Argonne National Laboratory, Argonne, IL, 60439, USA

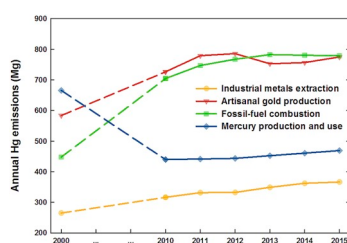
^b Department of Atmospheric Sciences, University of Washington, Seattle, WA, 98195, USA

^c Electric Power Research Institute, Palo Alto, CA, 94304, USA

^d Harvard John A. Paulson School of Engineering and Applied Sciences, Cambridge, MA, 02138, USA

^e Department of Environmental Health, Harvard T.H. Chan School of Public Health, Boston, MA, 02115, USA

GRAPHICAL ABSTRACT



ARTICLE INFO

Keywords:

Mercury
Emission trends
Concentration trends
Source contributions
Small-scale gold mining
Minamata Convention

ABSTRACT

Mercury (Hg) is a naturally occurring element in the Earth's crust. It can be harmful to human health when released in large quantities and/or converted to the neurotoxic methyl mercury in aquatic ecosystems. This study analyzes global and regional trends in anthropogenic Hg releases to the atmosphere between 2010 and 2015, as well as the associated trends in modeled and measured Hg concentrations at sites around the world. In general, we find that global Hg emissions and concentrations have grown slightly in this period, as declines from the phase-out of commercial Hg use in the developed world have been more than matched by increases in Hg-related activities in the industrializing countries of the world. We estimate that global Hg emissions between 2010 and 2015 have grown at a rate of 1.8%/yr, from 2188 Mg (+44%/-20%, 80% C.I.) in 2010 to 2390 Mg (+42%/-19%, 80% C.I.) in 2015. Regionally, emissions declined over this period in the U.S. (-10%), OECD Europe (-5.8%), and Canada (-3.2%), while they increased in Central America (+5.4%), South Asia (+4.6%), and Eastern Africa (+4.0%). East Asia remained the largest emitting region at 1012 Mg in 2015, though growth there has slowed significantly in recent years. The production of Hg (+7.9%), caustic soda (+6.3%), and cement (+6.3%) showed the highest increases by source type, though artisanal and small-scale gold mining (ASGM) was the single largest source of emissions in 2015 (775 Mg). The commercial use of Hg in dental applications (-5.6%) and electrical equipment (-5.2%) continued to decline. These emission trends show a continuation of the regional and sectoral shifts that began in the 1970s, but with a resulting reversal in global trends, because the

[☆] The submitted manuscript has been created by UChicago Argonne, LLC, Operator of Argonne National Laboratory (“Argonne”). Argonne, a U.S. Department of Energy Office of Science laboratory, is operated under Contract No. DE-AC02-06CH11357. The U.S. Government retains for itself, and others acting on its behalf, a paid-up nonexclusive, irrevocable worldwide license in said article to reproduce, prepare derivative works, distribute copies to the public, and perform publicly and display publicly, by or on behalf of the Government.

* Corresponding author.

E-mail address: dstreets@anl.gov (D.G. Streets).

<https://doi.org/10.1016/j.atmosenv.2018.12.031>

benefits from Hg phase-out in North America and Europe have been largely realized and industrial growth in developing countries has begun to dominate. The emission trends are in agreement with trends in modeled and measured concentrations, which show small declines in surface air total gaseous Hg concentrations in eastern North America and Western Europe between 2010 and 2015, but slight increases for much of the rest of the world, driven by the continued increases in emissions from Asia and from ASGM. Our results suggest that reductions of Hg in the North Atlantic region have been largely successful, and focus now needs to shift to Asia and to the continued practice of ASGM worldwide.

1. Introduction

It is well established that mercury (Hg) in the environment poses risks to the health of humans and wildlife, as described in the Global Mercury Assessment (GMA) (UNEP, 2013) and accompanying documentation (AMAP/UNEP, 2013). Natural releases of Hg to the atmosphere from the weathering of Hg-containing rocks, geothermal activity, and volcanism are relatively small—about 76–300 Mg/yr globally—while the bulk of the primary releases are associated with anthropogenic activities and amount to about 2000 Mg/yr (UNEP, 2013; Amos et al., 2015; Bagnato et al., 2014; Streets et al., 2011, 2017). For this reason, the Minamata Convention on Mercury was signed by 128 countries in 2013, calling for worldwide control of anthropogenic releases of Hg. Attention then turned to clarifying the source types and countries that are responsible for the release of Hg, as well as the options for its reduction and how the effects of the treaty might be evaluated (Evers et al., 2016; Giang et al., 2015; Gustin et al., 2016; Qiu, 2013; Selin, 2018).

For many environmental problems, local control of high-emitting sources is sufficient, but for Hg the situation is more complicated because: (a) the atmospheric lifetime of Hg against removal by deposition is ~6 months (Corbitt et al., 2011; Horowitz et al., 2017), allowing transport on a hemispheric-to-global scale; (b) mercury released to land can be transported into rivers and streams and find its way into lakes and oceans (Amos et al., 2014; Fisher et al., 2012); and (c) atmospherically deposited Hg can cycle through the surface environment in oceans, lakes, rivers, and soils and be re-emitted to the atmosphere. Thus, considerable mobilization and re-distribution of Hg occurs over time (Amos et al., 2013). Eventually, Hg is buried in estuarine or deep ocean sediment or stable terrestrial reservoirs, but the time scale for this sequestration ranges from decades to millennia.

Because of the mobility of previously-deposited Hg, we have studied historical Hg emissions in past work (Streets et al., 2011, 2017, 2018), but for implementing a control regimen, it is important to know the details of current emissions. No previous papers have attempted to generate annual emission trends for recent years, which is why we study a six-year period here, 2010–2015, with a common methodology for each year, and compare it with modeled and measured trends over the same period. In this way we can gain insight into the main contributing source types and world regions in the present time, as well as how their emissions are trending. It is hoped that this will guide implementation of the Minamata Convention and help to assess the likely benefits of any consequent emission reductions.

2. Data and method

In this work we estimate the amount of Hg released into the global atmosphere by human activities, annually for the six years in the period 2010–2015. In order to provide a guide for the trends that led up to this period, we also sometimes include estimates for earlier years made by the same method. The methodology follows previous work on long-term Hg emission trends (Streets et al., 2011, 2017; 2018; Horowitz et al., 2014). Because none of the previous work went beyond the year 2010, some updates to emission factors and source characterizations have been incorporated in the present work, as described below. We calculate emissions for 17 world regions (see Table si1 for the countries

in each region) and 17 source categories. Note that in previous work we included 18 source categories, but we find that Hg emissions from silver extraction are negligible in the 2010–2015 timeframe, so they are omitted from this analysis. There are four different approaches used to estimate emissions for the 17 source types, determined by the availability of activity data. In this section we divide the approaches into four types, based on the sources to which they are applied: (a) fossil-fuel combustion; (b) industrial metals production; (c) artisanal and small-scale gold mining (ASGM); and (d) production and uses of Hg in commercial products. These four approaches are described below in that order.

First, emissions from the combustion of fossil fuels are calculated using the latest annual energy statistics from the International Energy Agency (IEA), as of August 2017 (<https://www.iea.org/statistics/>). Emissions are calculated at the national level and then aggregated up to the 17 world regions. These energy statistics reflect a significant re-assessment of China's coal use in recent years (Liu et al., 2015; Korsbakken et al., 2016). Following earlier work (Bond et al., 2004, 2007; Streets et al., 2004), we disaggregate the IEA energy data into 144 sector/fuel/technology combinations (see Table 3 of Streets et al., 2004), each of which has a unique emission factor. Technology development over time is treated by transitions from simple to advanced systems. In recent work, we have added the use of flue-gas desulfurization (FGD) systems in the power sector (Streets et al., 2018); though primarily intended to capture SO₂, these systems also have a significant influence on Hg emissions. This is particularly important when calculating emissions after 2000, and especially for China, where there has been a remarkably rapid deployment of FGD since 2006 (Xu et al., 2009).

Second, emissions are calculated for the production of six industrial metals: copper, zinc, lead, iron, steel, and gold. As in our previous work (Streets et al., 2011, 2017), we use the following transformed normal distribution function to estimate the change of emission factor over time for each source type:

$$y_{r,p,t} = (a_{r,p} - b_{r,p})e^{(-t^2/2s_{r,p}^2)} + b_{r,p} \quad (1)$$

where

- $y_{r,p,t}$ = air emission factor in region r for process p in year t (g Mg⁻¹);
- $a_{r,p}$ = uncontrolled emission factor (g Mg⁻¹) in region r for process p ;
- $b_{r,p}$ = best emission factor achieved in region r for process p today (g Mg⁻¹); and
- $s_{r,p}$ = shape parameter of the curve for region r and process p .

By selecting values of the parameters a , b , and s to correspond to the known or inferred time development pathway of relevant technologies, we can estimate the value of emission factor y at any point in time t , reflecting the improved performance of processes and/or the addition of pollution control technology, averaged over all installations region-wide. Five regional groupings are used to reflect variations from the most highly developed and environmentally proactive regions to poorly developed regions with few attempts to limit pollutant releases (Streets et al., 2011). Because previous work did not go beyond 2010, we performed an initial review of pollution control initiatives in the past

decade to see if modifications to the previous curves were necessary for any source type in any of our 17 world regions. As a result, we determined that it was necessary to modify emission factors determined by the above method for copper and zinc smelting in China for the years 2010–2015, in order to reflect transformational changes in these industries in the past decade. Wu et al. (2012) reviewed Hg emissions from China's primary metal smelters and concluded that emission factors used previously were out of date because of the rapid phase-out of artisanal smelters and the addition of more-efficient pollution control devices. They recommended lower values, which were subsequently incorporated into anthropogenic Hg emission estimates for China (Zhang et al., 2015; Huang et al., 2017). We therefore lowered our estimates for the East Asia region to 2 g Hg/Mg Cu produced and 11.5 g Hg/Mg Zn produced for the year 2010 and later years. Annual activity levels for the industrial metals production group were obtained from United States Geological Survey (USGS) statistics (<https://minerals.usgs.org/minerals/pubs/commodity/myb/>) at the national level and aggregated to the 17 world regions.

The third source category is ASGM. Developing trends in emissions of Hg from ASGM is a major challenge. To date, there is only one reliable point estimate, made by the GMA (UNEP, 2013; AMAP/UNEP, 2013), which is for the year 2010. Of course, even that value has significant uncertainty due to incomplete knowledge of the extent of ASGM activities around the world. The GMA estimated global Hg emissions from ASGM in 2010 to be 727 Mg with an uncertainty range of 410–1040 Mg. We have used that value in our previous work (Streets et al., 2017), though our uncertainty range (80% C.I., based on Monte Carlo simulations) is slightly narrower, 490–970 Mg (see Fig. 1).

Trending the value of 727 Mg to other years in the range 2010–2015 can only be done using proxy information, because there are presently no other estimates for years after 2010, and estimates for earlier years are acknowledged to be incomplete and highly uncertain. Muntean et al. (2014) used trends in large-scale gold production (what we described above as industrial gold production) from Telmer and Viega (2008) to construct ASGM estimates for the period 1970–2008. For this work, we tested six plausible proxies: (a) regional industrial gold production, as per Muntean et al. (2014), but using the 2010 GMA national estimates from UNEP (2013) and AMAP/UNEP (2013)); (b) global industrial gold production (UNEP, 2013; AMAP/UNEP, 2013); (c) gold price (<http://onlygold.com/Info/Historical-Gold-Prices.asp>); (d) world gold demand (<https://www.gold.org/search/site/historical%20gold%20demand?page=4>); (e) excess gold demand (gold demand minus

industrial gold production); and (f) mercury production (UNEP, 2017). The last one is not expected to be a very good proxy, however, because of other uses of the produced Hg—even though any major changes, especially increases, in Hg production are likely associated with ASGM. Each of those proxy data series was used to trend the 2010 GMA value back to 2000 and forward to 2015. The results are shown in Fig. 1.

Application of our methodology suggests that growth in Hg emissions from ASGM has slowed since 2010 but not halted. The annual growth rate from 2000 to 2010 was about 2.2%/yr, based on our 2000 value of 584 Mg (Streets et al., 2017), or 3.8%/yr using the 2000 value of Muntean et al. (2014) of 499 Mg. Taking the average of all proxies used, we estimate that the growth rate between 2010 and 2015 had slowed to 1.3%/yr. We estimate a peak value of 786 Mg in 2012, declining slightly to 775 Mg by 2015. As Fig. 1 shows, the moderation of the increase was driven primarily by lower world gold prices and reduced excess gold demand. This analysis suggests that ASGM is still a major contributor to global atmospheric Hg emissions, but that its influence may (hopefully) have peaked. If interventional measures to reduce ASGM and/or substitute lower-emitting techniques (Fritz et al., 2016; Seccatore et al., 2014; Veiga et al., 2014) have been widely successful, then it is possible that the increase in ASGM emissions could have been less since 2010, or even that ASGM emissions are now definitely declining; new surveys of country-specific initiatives and their effectiveness are urgently needed to confirm or refute this notion. For this work, we use the proxy-trended annual average values for ASGM emissions for 2010–2015, anchored to the GMA 2010 value. For each proxy in each year, we calculate its value relative to the year 2010. We then calculate a simple average across all six proxies for each year to obtain the proxy averages. Fig. 1 shows the values for 2010–2015 plus the years 2000 and 2008 for reference; these eight years are the only ones for which we have values for all six proxies. Note that the range of the proxy values is smaller than the uncertainty ranges for the year 2010 emissions estimated in either this work or the GMA, as shown in Fig. 1. In addition to uncertainty in the amount of ASGM taking place, further refinement is also needed on the fraction of Hg released to the atmosphere during ASGM, as well as the Hg⁰/Hg fraction in air emissions, in typical real-world operating environments around the world.

The fourth and final category of Hg emissions is associated with the production and uses of Hg in commercial products. We use year-2010 and year-2015 data on regional-level Hg consumption by sector (UNEP, 2017) to estimate year-2015 emissions from this category. We then scale year-2010 regional emissions estimates (Streets et al., 2017) from

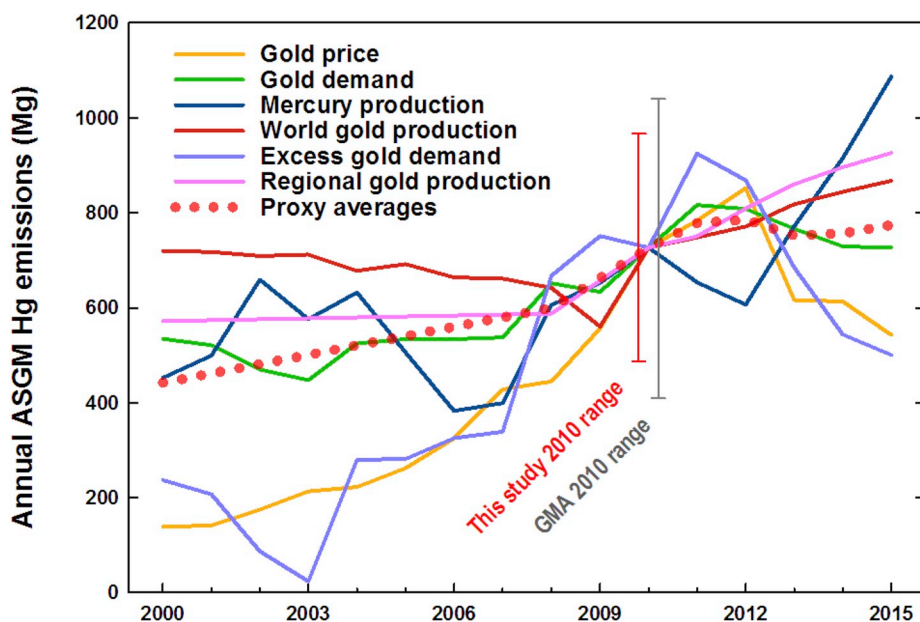


Fig. 1. Estimates of annual Hg emissions (Mg) from Artisanal and Small-Scale Gold Mining (ASGM) obtained by trending the 2010 value from the GMA (UNEP, 2013; AMAP/UNEP, 2013) to other years in the period 2000–2015 using six alternative proxies. The average of all proxies is shown as the dotted red line. Also shown are the uncertainty ranges for the 2010 value estimated in this work and the GMA. (For interpretation of the references to colour in this figure legend, the reader is referred to the Web version of this article.)

each sector (caustic soda production, chemicals manufacturing, electrical and measuring equipment, and dental applications) by changes in the regional consumption of Hg for each sector. This implicitly assumes the same emission factors for year 2015 as in year 2010 from Streets et al. (2017). For municipal waste and other waste burning, we scale year-2010 regional emission estimates by the change in total Hg consumption in Hg-added products (and hence potential Hg-containing waste) from the year 2010–2015 (UNEP, 2017). Between 2010 and 2015, emissions are then interpolated to annual estimates.

We also estimate in this work the fraction of global anthropogenic Hg emissions to the atmosphere that is released as elemental Hg (Hg⁰), because this has important implications for the balance between local deposition and long-range transport in each geographical region and the trend in that balance over the six years of this study. We think that if the changes in the Hg⁰/Hg ratio are significant they could at least partially explain trends in observations over the same time period. We use the same source-specific Hg⁰ fractions as in previous work (Streets et al., 2017, 2018).

3. Results and analysis

We organize our results into four sections, in order to give insight into the forces driving Hg emissions in recent years. Because our baseline calculations are performed for 17 source categories in each of 17 world regions for each of six years (see Tables 1 and 2 for detailed estimates, including the year 2000 for comparison), it requires selective aggregation to understand why the trends have the structure that they do. Previous studies investigating observed Hg trends have tended to compare them against only regional emission trends; here we also investigate the impacts of global Hg trends and changes in speciation. This section discusses, in order, sectoral, regional, global, and speciation trends in Hg emissions.

3.1. Sectoral emission trends

Fig. 2 shows global trends over the period 2010–2015 for the four aggregated source categories of Hg emissions referred to above, with reference to emissions in the year 2000 (Streets et al., 2017). Emission values for the aggregated source categories and their composition are shown in Table si2. Three of the four categories show overall growth in the period 2000–2015: fossil-fuel combustion (3.8%/yr), industrial metals extraction (2.2%/yr), and ASGM (1.9%/yr). This is consistent with continued expansion of the global economy, but it is less than the growth in world GDP over the same period (5.7%/yr) (<http://www.imf.org>), suggesting continuous improvement in pollutant emissions per

unit of production. The growth rate slowed for the period 2010–2015 in fossil-fuel combustion (2.0%/yr), aided in large part by the widespread introduction of FGD on coal-fired power plants in China. It also slowed for ASGM (1.3%/yr), as previously discussed. However, emissions from industrial metals extraction increased to 3.0%/yr, as Asian economies like China and India rapidly expanded industrial production.

The fourth category, mercury production and use, shows a continuation of the decline that began ca. 1970 (Horowitz et al., 2014), at a rapid rate of 4.1%/yr, until 2010. This was due to phase-out of the use of Hg in industrial processes, electrical devices, etc., particularly in the developed world. However, it appears that several years prior to 2010, emissions from this source category bottomed out, and a slow increase commenced (1.3%/yr), perhaps reflecting the completion of phase-out of the easy Hg-replacement options in the developed world and slow growth of Hg use in the industrial expansion of developing countries. Fig. 2 also shows the slow, continued, growth in Hg emissions from ASGM. Our analysis suggests that annual Hg emissions in this source category grew from 584 Mg in 2000 to 727 Mg in 2010 and 775 Mg in 2015.

As Table 2 shows, the largest sectoral increases in global Hg emissions during 2010–2015 were in mercury production (7.9%/yr), caustic soda production (6.3%/yr), and cement production (6.3%/yr). The largest decreases in emissions were in dental applications (−5.6%/yr), electrical equipment (−5.2%/yr), and oil combustion (−0.2%/yr). In 2015, Hg emissions were still dominated by ASGM (775 Mg), coal combustion (558 Mg), and cement production (206 Mg).

3.2. Regional emission trends

Fig. 3 shows the same types of trends as Fig. 2, but this time disaggregated into the seven major world regions. There has been a continuation of the reduction in Hg emissions in the North Atlantic region (defined for this purpose as North America, OECD Europe, Eastern Europe, and the Former Soviet Union) that began in about 1970. For the complete period from 2000 to 2015, emissions declined by 4.6%/yr in North America and by 3.5%/yr in Europe and the Former Soviet Union. Little change is evident in South America. Emissions in Africa and the Middle East remained high, with a slight increase of 1.3%/yr, due to continued expansion of ASGM, as discussed previously. Asia showed the greatest change, particularly East Asia (4.3%/yr increase) and South Asia (3.1%/yr increase). In the rest of Asia and Oceania there was a slight decline in emissions of 1.1%/yr.

Emissions for the Asian regions are acknowledged to be uncertain. For South Asia, our estimate for 2010 (153 Mg) is very similar to that of the GMA (154 Mg) (UNEP, 2013). However, a comprehensive study of

Table 1
Annual emissions of mercury by world region (unit: Mg/yr).

World region	2000	2010	2011	2012	2013	2014	2015	2010–2015 growth (%/yr)
Canada	12.7	9.8	9.1	8.7	8.6	8.7	8.3	−3.16
USA	127.7	73.1	66.9	59.1	55.5	50.6	42.7	−10.19
Central America	33.5	26.4	29.6	31.1	32.1	33.1	34.3	5.42
South America	239.0	266.0	279.5	279.6	270.9	271.5	275.8	0.73
Northern Africa	38.0	14.0	14.4	15.2	15.1	15.8	16.3	3.13
Western Africa	111.3	163.9	177.4	183.2	182.4	189.0	193.7	3.41
Eastern Africa	19.1	59.9	65.8	69.9	69.9	70.7	72.9	4.00
Southern Africa	147.6	106.9	108.5	110.8	109.7	112.3	112.8	1.09
OECD Europe	106.2	51.2	49.3	48.1	44.7	40.9	38.0	−5.77
Eastern Europe	49.4	35.9	37.8	35.8	34.4	33.5	33.6	−1.31
Former USSR	114.9	85.1	87.8	88.2	86.6	85.5	86.4	0.30
Middle East	49.3	39.3	41.7	43.8	43.1	45.4	46.3	3.36
South Asia	120.8	153.3	160.7	169.3	174.9	184.6	191.6	4.56
East Asia	532.7	901.4	961.2	973.9	997.3	1002.3	1012.3	2.35
Southeast Asia	224.6	168.2	176.1	178.6	176.7	180.6	187.5	2.19
Oceania	28.6	25.7	26.4	26.7	27.1	27.6	28.8	2.35
Japan	8.8	8.1	7.9	8.2	8.4	8.4	8.3	0.57
Global Total	1964.1	2188.0	2300.2	2330.0	2337.4	2360.5	2389.8	1.78

Table 2
Annual emissions of mercury by source category (unit: Mg/yr).

Source category	2000	2010	2011	2012	2013	2014	2015	2010–2015 growth (%/yr)
Copper smelting	57.3	59.7	62.4	62.8	65.2	69.8	70.0	3.23
Zinc smelting	81.7	96.4	98.2	90.1	95.3	98.2	103.6	1.44
Lead smelting	16.7	25.2	28.0	29.0	28.0	28.4	25.6	0.36
Iron manufacturing	22.1	38.2	40.9	41.7	44.0	44.4	43.4	2.60
Steel making	4.8	9.9	10.4	10.6	11.6	12.0	11.7	3.48
Mercury production	36.4	22.6	20.4	18.9	23.8	28.1	33.0	7.87
Gold, large-scale	82.7	87.1	91.9	98.1	104.9	109.4	112.1	5.18
Gold, ASGM	583.7	726.8	779.4	786.1	752.9	757.1	775.1	1.30
Cement production	74.3	151.9	168.5	177.1	188.6	192.8	206.3	6.31
Caustic soda	44.5	14.8	15.9	16.9	18.0	19.1	20.1	6.31
Coal combustion	359.9	538.2	564.4	576.1	580.1	573.6	558.3	0.74
Oil combustion	13.7	14.4	14.4	14.5	14.3	14.2	14.3	-0.22
Municipal waste	202.6	124.3	127.6	130.8	134.1	137.4	140.6	2.50
Other waste burning	201.9	149.3	152.6	155.8	159.1	162.3	165.6	2.09
Electrical equipment	118.7	81.1	77.3	73.5	69.7	65.9	62.0	-5.22
Chemicals	13.9	26.4	27.5	28.6	29.6	30.7	31.8	3.74
Dental	49.4	21.5	20.4	19.3	18.3	17.2	16.1	-5.60
Global Total	1964.1	2188.0	2300.2	2330.0	2337.4	2360.5	2389.8	1.78

Hg releases in India has somewhat higher values, including an estimate of emissions to air of 236 Mg in 2010 (Chakraborty et al., 2013), which nevertheless is well within the GMA uncertainty range of 78–358 Mg. Detailed studies of Hg flows in all aspects of economic activity, such as Chakraborty et al. (2013), can be very valuable in refining emission estimates—and they often lead to higher estimates arising from missing source types or underestimated emission rates. More such national studies are needed to improve the accuracy of global estimates.

The declines on both sides of the North Atlantic are reflected in measurement trends recorded at sites in North America and Europe, as shown later in this paper. However, they should not be considered to be representative of recent global trends, as Fig. 3 shows. For example, the combined emissions in the North Atlantic region in 2015 (243 Mg) are only a quarter of the emissions in East Asia alone (1021 Mg). The ray of hope on the horizon is that the increasing trend of Hg emissions in East Asia slowed considerably since 2010, down to 2.3%/yr, due to the widespread installation of FGD systems on coal-fired power plants in China. Counteracting this improvement, however, is the observation that Hg emission trends in South Asia have risen faster since 2010, at a rate of 4.6%/yr, because of large-scale expansion of coal use without

effective emission controls.

Table 1 shows that the largest regional increases in Hg emissions during 2010–2015 were in Central America (5.4%/yr), South Asia (4.6%/yr), and Eastern Africa (4.0%/yr). The largest decreases were in the U.S. (-10.2%/yr), OECD Europe (-5.8%/yr), and Canada (-3.2%/yr). In 2015, Hg emissions were the highest in East Asia (1012 Mg), South America (276 Mg), and Western Africa (194 Mg).

3.3. Global emission trends

Tables 1 and 2 summarize the annual Hg emission estimates for the study period 2010–2015, as well as the year 2000 for comparison. The estimates reveal that global Hg emissions continued to grow throughout the study period, from 2188 Mg in 2010–2390 Mg in 2015, a growth of 9.2% over the entire period, or a growth rate of 1.8%/yr. This represents an increase over the growth rate for the period 2000–2010, which was 1.1%/yr, aided by the economic recession of the late 2000s and the continued decline of commercial Hg production and use. As we discuss in Sec. 4, the 2010–2015 increasing trend in global Hg emissions is a reversal of the declining trend in global emissions from ca

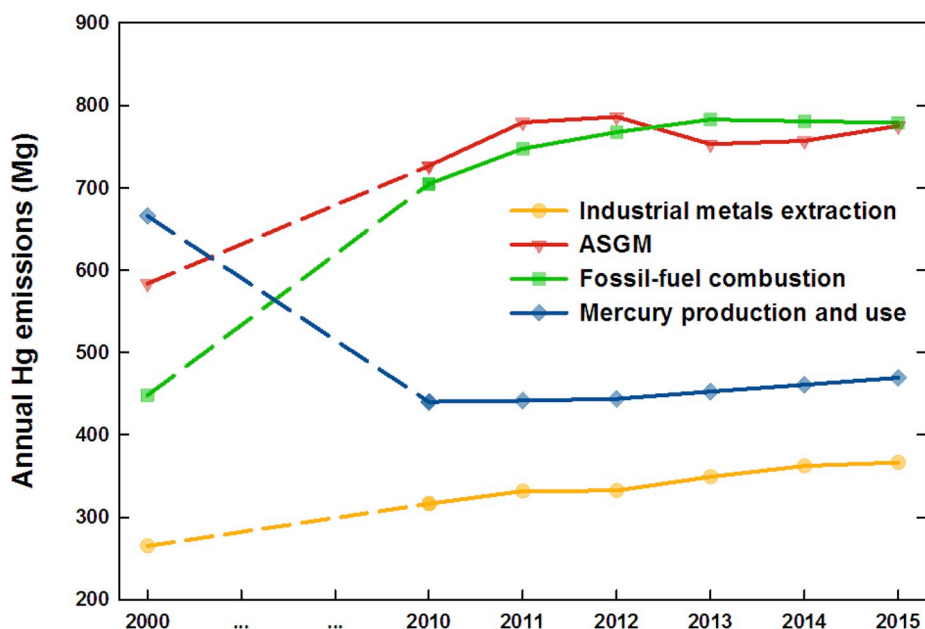


Fig. 2. Emissions of Hg (Mg/yr) from four aggregated source categories for the period 2010–2015, with the year-2000 values shown for comparison.

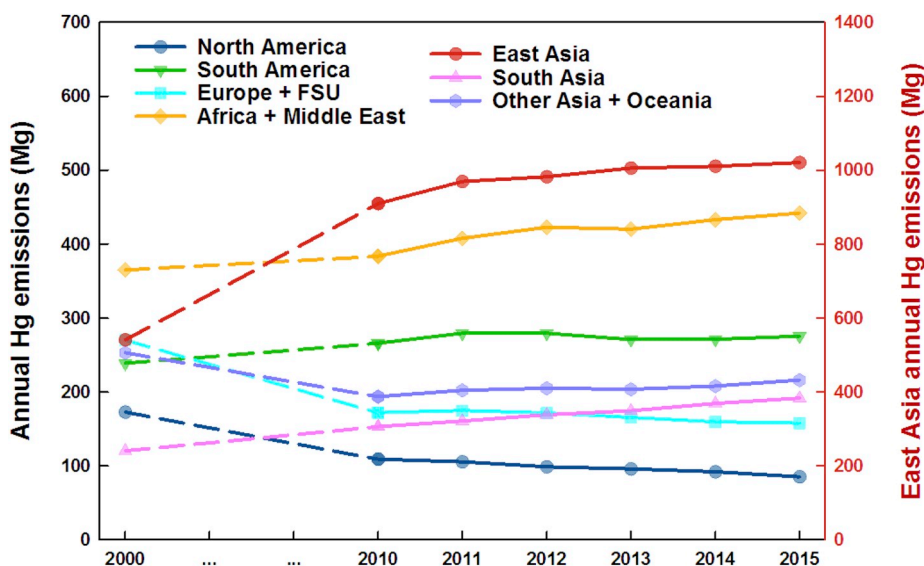


Fig. 3. Emissions of Hg (Mg/yr) from seven world regions for the period 2010–2015, with the year-2000 values shown for comparison. Note that the scale for the East Asia trend is doubled in order to make the trends in all regions clearly visible.

1970 to the late 2000s that was reflected in declines in measured Hg concentrations at most sites during this period.

In comparison with other studies, our reference global emission estimate for the year 2010 in this work, 2188 Mg, which is slightly lower than the value of 2270 Mg reported in Streets et al. (2017) because of the adjustment of China's smelting emissions reported in Sec. 2, is higher than the GMA value of 1960 Mg (UNEP, 2013; AMAP/UNEP, 2013). A recent estimate of 2010 emissions from the EDGARv4.tox2 Hg inventory (Muntean et al., 2018), on the other hand, is 10% lower than the GMA inventory for matching sectors. All three of these estimates are well within the GMA uncertainty range for global Hg emissions of 1010–4070 Mg (UNEP, 2013; AMAP/UNEP, 2013), illustrating just how challenging it is to quantify Hg emissions from many economic sectors and regions of the world that do not have transparent characterizations of technology and activity levels.

Fig. 4 presents a pictorial summary of trends during the period

2010–2015 for Hg emissions in important regional components of the global situation, compared with trends in selected key factors that influence the releases of Hg to the atmosphere. The increase in global Hg emissions was less than the growth in global GDP (5.2%/yr (IMF, 2018) and global industrial production (2.0%/yr (World Bank, 2018), but more than the growth in global population (1.2%/yr (United Nations, 2017). Fig. 4 shows that South Asia (essentially India) has taken over from East Asia (essentially China) as the fastest growing region for Hg emissions (4.6%/yr vs. 2.3%/yr); this is consistent with similar trends in SO₂ emissions (Li et al., 2017). ASGM is still a large contributor to total emissions, but it is no longer growing as fast as it once was (1.3%/yr) and declining since 2013. It is clear that emissions in the North Atlantic region continue to decline (−4.4%/yr), aided mostly by reductions in the production and uses of Hg for commercial applications (−2.0%/yr). While this is a significant and

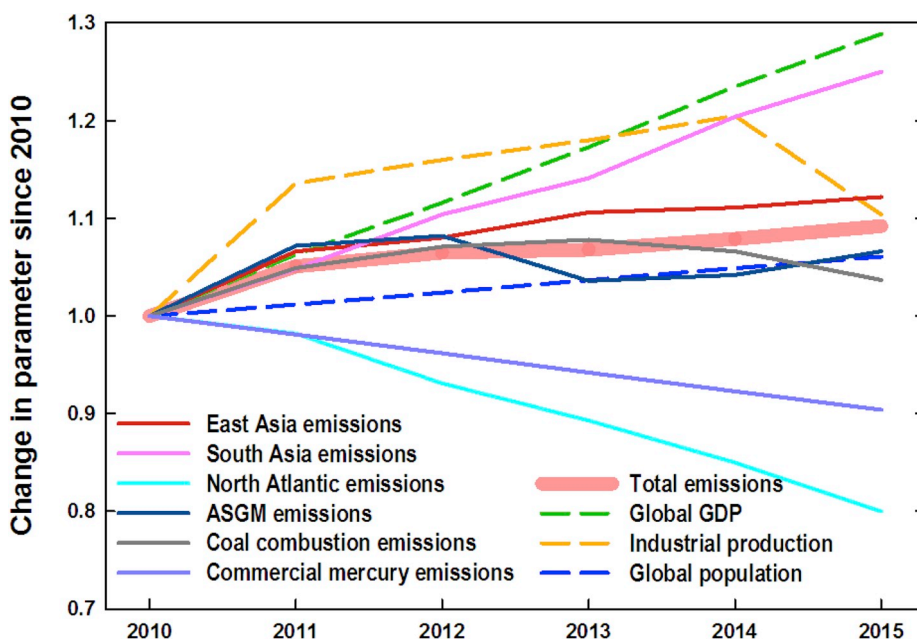


Fig. 4. Key trends (2010 = 1) in Hg emissions and related factors for the period 2010–2015.

beneficial decline, it should not be considered to be representative of global trends; the absolute value of Hg emissions in this region is now heavily outweighed by Asian emissions, as discussed later in this paper.

3.4. Elemental mercury trends

Thus far, the emission trends discussed in this paper have been concerned with total Hg emissions to the atmosphere, but it is also important to examine the trends in emissions of divalent Hg and elemental Hg. The former has a lifetime of days to weeks, compared to many months for the latter (Corbitt et al., 2011; Horowitz et al., 2017). If the fraction of total Hg emitted as Hg⁰ changed during the period 2010–2015, then the balance between long-range Hg transport and local Hg deposition will have changed commensurately. This has important implications for trends in measured Hg concentrations. In this work we calculated Hg⁰ emissions as in previous work, for each source type separately (Streets et al., 2017, 2018). The results are shown in Fig. 5, which presents the change in the Hg⁰/Hg fraction since 2010, globally and for key world regions and source categories. These fractional changes would need to be combined with the absolute values of Hg emissions for each component in order to determine whether the changes are significant or not at global or regional level.

Over the six-year period we find negligible change in the global fraction of Hg⁰ in total Hg. The fraction has remained stable at ~0.69 throughout the six-year period. However, there have been changes in key regions and source categories. We find that the fraction has increased in North America (2.3%/yr) and Europe (0.7%/yr), which is consistent with earlier findings reported by Zhang et al. (2016) for the period 1995–2010. We attribute these increases to ongoing region-wide reductions in emissions of Hg from industrial operations; divalent and particulate Hg are captured, while Hg⁰ is not. Thus, the fraction of Hg⁰ increases over time and long-range transport of Hg is favored over local deposition in the North Atlantic area. The fractions of Hg⁰ in emissions in South Asia and East Asia have grown only slightly, each by 0.1%/yr.

Certain sources of Hg have changed their Hg⁰/Hg fractions as a result of technological transformations and/or the implementation of emission controls. Coal combustion emissions worldwide have seen a greater increase in the Hg⁰ fraction (0.4%/yr), due in large part to the widespread use of FGD in China. Commercial Hg emissions have shown the largest change (3.2%/yr increase) from 0.74 to 0.87. This is due to the elimination or major reduction in the uses of Hg in industrial

chemical operations. What remains currently is largely the use of Hg in commercial products like electrical and measuring equipment, dental applications, etc., and thus the fraction of Hg⁰ trends rather quickly towards the value of 1 for this source category.

3.5. Uncertainty in emission estimates

We performed an uncertainty analysis for the 2010–2015 emission estimates, following the method initially developed for China (Wu et al., 2010) and subsequently expanded for global emissions (Streets et al., 2011) that uses a Monte Carlo framework of 10,000 simulations and uncertainty estimates for all emission factors and activity levels. Fig. 6 shows the uncertainty bounds for total Hg releases in this work, expressed as 80% confidence intervals (C.I.) surrounding the central estimates. This means that the probability of releases being outside the calculated range is 20% or less. The uncertainty range is relatively unchanged throughout the period, falling slightly from +44%/–20% in 2010 to +42%/–19% in 2015, driven by the changing mix of source types. The range is somewhat larger than it was in the year 2000 (+38%/–18%), due to the increasing role of ASGM and the high uncertainty in emission factor and activity level associated with it. De Simone et al. (2017) examined the propagation of emissions uncertainty through global transport models to uncertainty in deposition estimates, concluding that the uncertainty in deposition flux is high, because of the significant contribution of remote source regions to total deposition in many receptor regions.

4. Observed and modeled trends

The emissions calculated in this work are shown in Fig. 7A and B, with sub-regional spatial distributions from Zhang et al. (2016). Results show a continued decline in anthropogenic Hg emissions in North America and Europe between 2010 and 2015. We then modeled the corresponding change in surface air concentrations of total gaseous mercury (TGM) using the emissions from this work and the GEOS-Chem global atmospheric Hg simulation model (Horowitz et al., 2017; <http://geos-chem.org>) (Fig. 7C and D). Results show small declines in surface air TGM concentrations in eastern North America and Western Europe between 2010 and 2015, where most emission reductions are occurring, but slight increases for much of the rest of the world driven by the continued increases in emissions from Asia and ASGM. Observed

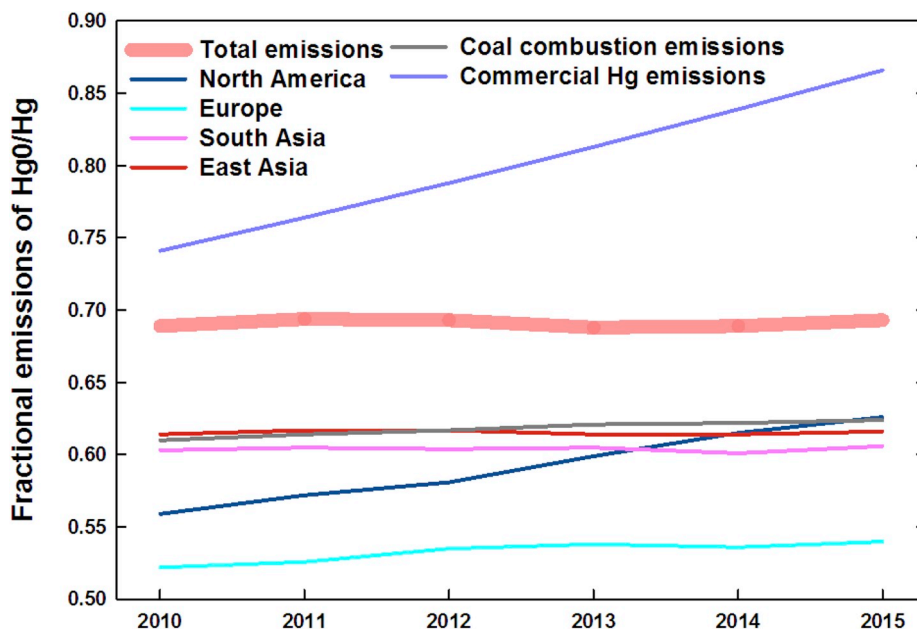


Fig. 5. Trends in the Hg⁰/Hg fraction in atmospheric Hg emissions from major world regions and key source types for the period 2010–2015.

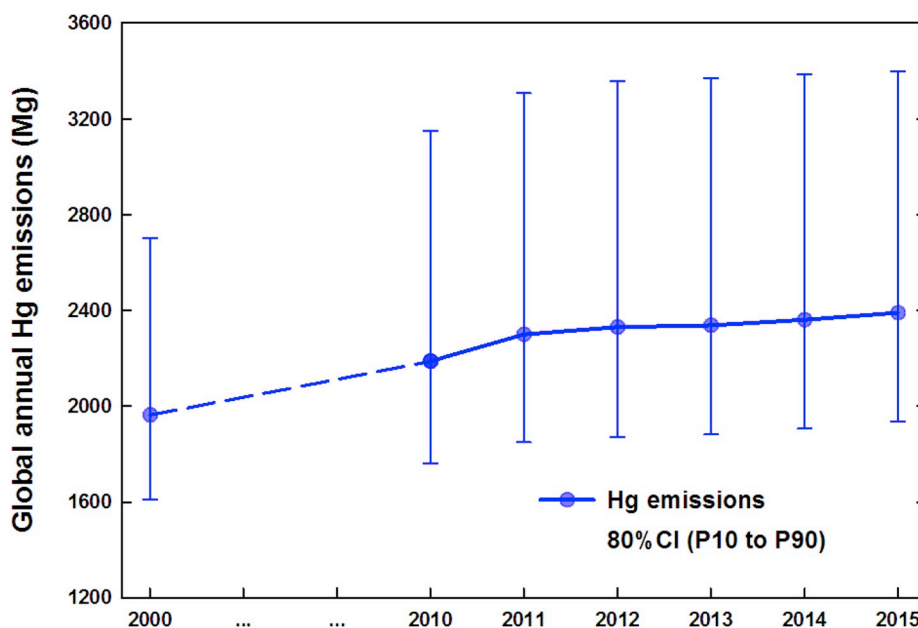


Fig. 6. Uncertainty bounds of total Hg release estimates (Mg/yr) for 2000 and 2010–2015, showing 80% confidence intervals (C.I.) around the central estimates.

declines in eastern North America surface air TGM concentrations between 2010 and 2015 are clearly flatter than the emission trends between 2010 and 2015 (i.e., $-4.4\%/yr$ for North America) and increase in some parts of the region due to the increasing contribution of global background TGM to surface air as regional emissions decline. The largest increases in surface air TGM between 2010 and 2015 are apparent

in Asia and can be attributed to continued growth in emissions from industrial metals extraction ($4\%/yr$) and coal combustion ($2\%/yr$) in China.

Global anthropogenic Hg emissions estimated in this study increased by $1.8\%/yr$ between 2010 and 2015, mainly due to continued increases in Asia and the ASGM sector globally. In prior work, we found

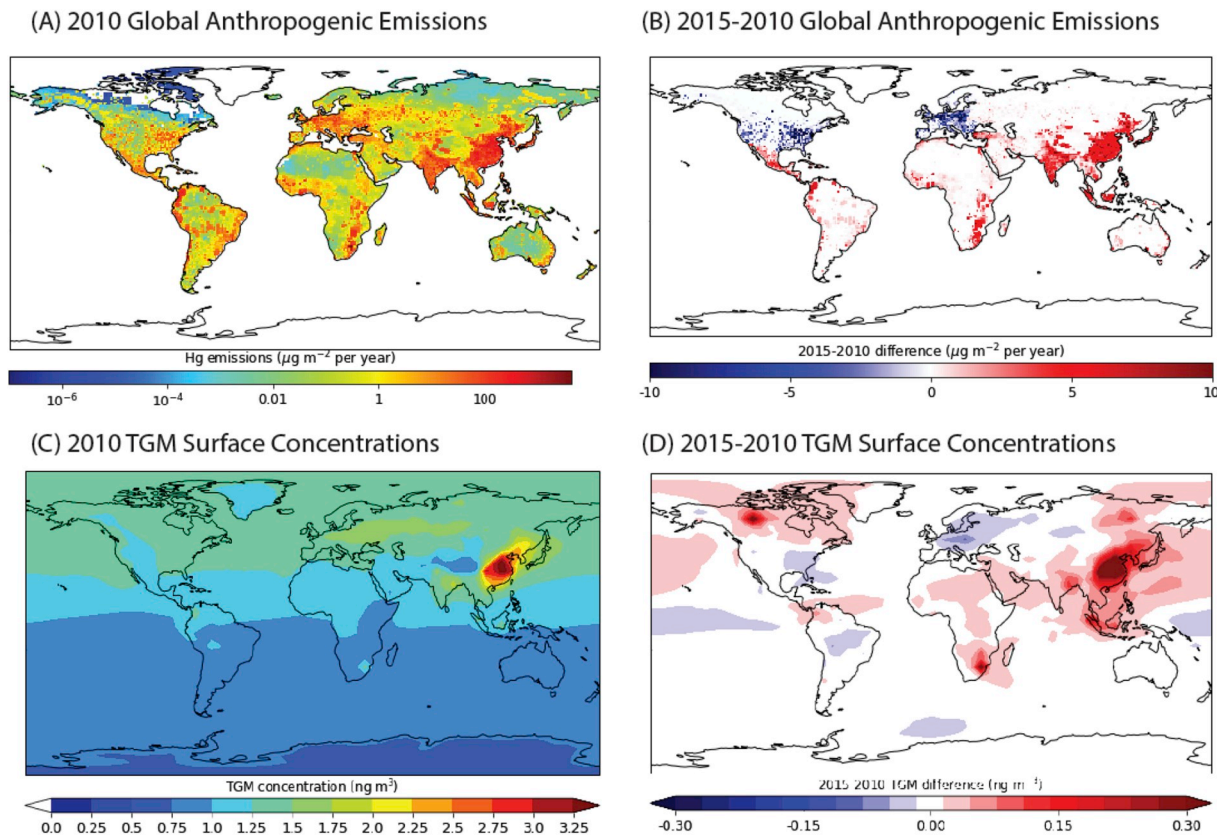


Fig. 7. Global anthropogenic Hg emissions and corresponding simulated surface total gaseous mercury (TGM) concentrations based on the GEOS-Chem global chemical transport model (Horowitz et al., 2017). Panels (A) and (C) show anthropogenic emissions and surface concentrations for the year 2010. Panels (B) and (D) show the differences between 2015 and 2010 emissions and surface concentrations of TGM, respectively.

an increase of 1.1%/yr between 2000 and 2010 (Streets et al., 2017). TGM concentrations measured in the free troposphere provide a good indication of global background concentrations. Observations between 2010 and 2015 indicate a slight increase in concentrations at the Mauna Loa Observatory in Hawaii of $1.2 \pm 2.0\%/yr$, but this trend is not statistically significant (Fig. 8A). For the CARIBIC commercial flight data, which includes continental Europe, North America, and the North Atlantic, there is a slight decrease of $-0.60 \pm 0.58\%/yr$ between 2010 and 2015, but this is also not statistically significant (Fig. 8A). The CARIBIC measurements are from repeated aircraft measurements, while the Mauna Loa data are from a long-term monitoring station, so we think this data set is a good indicator of global background. Observed trends in free tropospheric TGM reflect a combination of primary anthropogenic emissions and re-emissions from terrestrial and aquatic surfaces. Jiskra et al. (2018) recently proposed that increased terrestrial primary productivity and associated vegetative uptake of Hg^0 in the Northern Hemisphere over the last 20 years has contributed to the observed decline in TGM. This may have offset some of the global Hg emission increases in recent years suggested by the present work.

Anthropogenic emissions of Hg declined substantially in North America (4.6%/yr) and Europe (3.5%/yr) between 2000 and 2015. Clear evidence of corresponding declines of surface air TGM concentrations in these regions is apparent in the observations (Fig. 8B and C). However, surface air TGM concentrations from long-term monitoring stations between 2010 and 2015 suggest that decreases in North America and Western Europe may be leveling off in recent years (Fig. 8B and C). Similar to results shown in Fig. 7C and D, these observations suggest that regional trends have been offset by continued increases in global emissions between 2010 and 2015.

Observed patterns in surface air TGM concentrations (Fig. 8B and C) are consistent with the conclusions of several prior studies, which suggest that observed declines in surface air TGM concentrations in the late-1990s began to reverse in the mid-to-late 2000s. For example, Weiss-Penzias et al. (2016) found declines in atmospheric TGM concentrations at most sites in the U.S. between the late 1990s and mid-2000s. However, between 2007 and 2013 trends were more mixed across the country with declines in TGM in some regions of the Eastern U.S. and increases among some sites in the Midwestern and Western U.S (Weiss-Penzias et al., 2016). Martin et al. (2017) reported a downward trend in TGM concentrations at Cape Point, South Africa, between 1995 and 2005 and an upward trend between 2007 and 2015. Ebinghaus et al. (2011) reported decreases of 1.6–2.0%/yr between 1996 and 2008 at Mace Head, Ireland; and Weigelt et al. (2015) noted slower declines in later years (up to 2013) that were steeper for polluted European air masses than sub-tropical maritime air. Read et al. (2017) found a decreasing trend in TGM of $-4.2 \pm 3.3\%/yr$ between 2011 and 2015 at Cape Verde, a remote sub-tropical Atlantic site. Tang et al. (2018) reported recent trends of atmospheric Hg in East China that showed a decline in GEM concentrations between 2014 and 2016, in contrast to reported continuous increases up to 2012 (Fu et al., 2015). This recent decline is attributed to air pollution control policies that targeted SO_2 , NO_x , and PM, and had co-benefits for Hg control. These policies have been most effective in the more highly developed regions of China, like the Yangtze River Delta where the measurements of Tang et al. (2018) were taken. This is consistent with our emission trends that show a leveling off of Hg emissions in the entire East Asia region by 2015 (Table 1 and Fig. 3).

5. Conclusions for policy development

The emission trends reported in this work for the period from 2010 to 2015 have implications for the development of national, regional, and global policies, including implementation of the Minamata Convention. We summarize in Fig. 9 the most significant trends that have driven global emissions over the past 50 years. Increasing industrialization after World War II drove a steady increase in global Hg emissions that peaked around

the year 1970 (blue line in Fig. 9). Along the pathway from 1950 to 1970, the North Atlantic region (the U.S. and Western Europe, primarily) was driving the increases (green line in Fig. 9). Between 1960 and 1970, increasing awareness of the deleterious impacts of Hg in the environment began to influence emission control policies and the intentional use of Hg. This effect, however, was largely experienced in the North Atlantic region, where emissions declined rapidly after 1970, illustrating the success of stringent regulations. The global decline was less dramatic due to the contributions from other world regions. After 1980 or thereabouts, emissions in Asia and Oceania (China and India, primarily) began to grow rapidly. In contrast to these two extreme and opposing trends, Hg emissions in the rest of the world remained relatively flat throughout the period. Our results for the period 2010–2015 show that the decline in the North Atlantic region and the increase in the Asia region have both leveled out considerably. Fig. 9 shows how the roles of the North Atlantic and Asia regions in releasing Hg into the environment have dramatically reversed in the last 50 years. This shift is largely reflected in the atmospheric Hg concentration measurements taken at sites around the world and in the simulations of atmospheric concentrations by chemical transport models. These regional trends, in combination, resulted in a downward trend in global releases to the atmosphere since 1970 that likely ended in the late 2000s and was replaced by a slow increase thereafter; however, we find that the increase had flattened out considerably by 2015. We conclude that at present we are in a period of relative stasis in the input of Hg into the atmospheric environment, and more action is needed to drive further decreases in atmospheric concentrations.

The implications for control policies are clear. The phase-out of

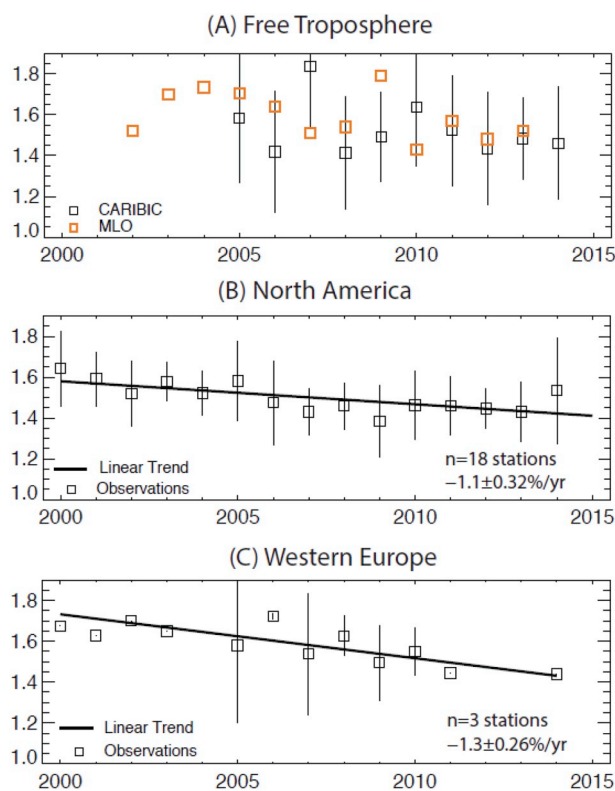


Fig. 8. Measured concentrations of TGM in the atmosphere and linear trends inferred from an ordinary linear regression on the annual means (only significant trends are shown). Data for the free troposphere are from the Mauna Loa Observatory (MLO) in Hawaii and the CARIBIC commercial flight data (www.caribic-atmospheric.com), as summarized in Zhang et al. (2016). North American atmospheric data are from the CAMNet (<https://www.ec.gc.ca/natchem>) and AMNet (nadp.sws.uiuc.edu/amn) networks and the Experimental Lakes Area, Canada. Observations in Western Europe are from the EMEP network (www.emep.int) and Global Mercury Observing System (GMOS) data from Sprovieri et al. (2016).

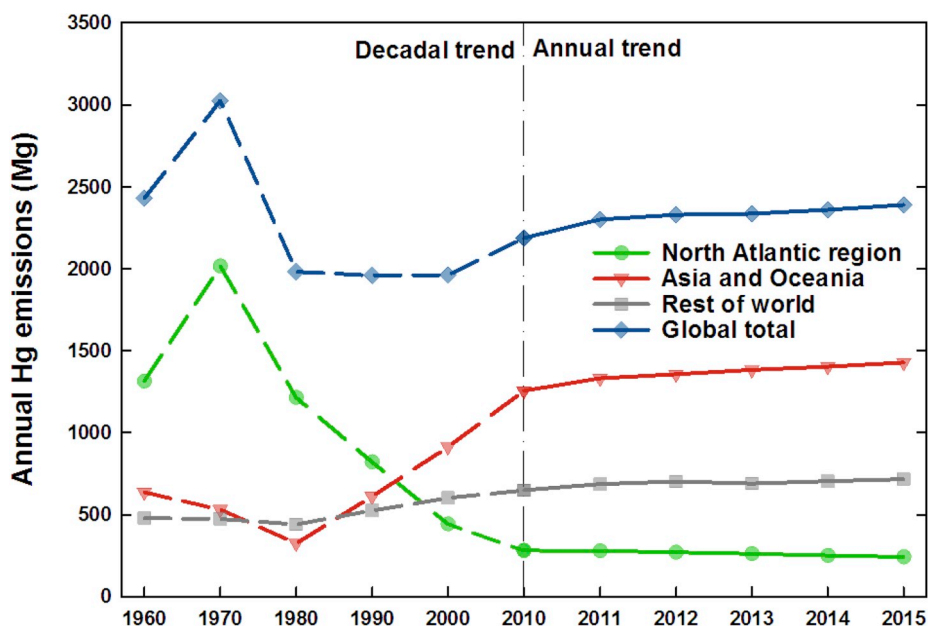


Fig. 9. Long-term trends in Hg emissions (Mg/yr), globally and in three sub-regions of the world, for the period 1960–2015. The left side of the graph shows the decadal trend for 1960–2010 (from Streets et al., 2017), while the right side shows the annual trend for 2010–2015 from this study.

mercury use in products and processes in the North Atlantic region has been very successful. Accompanied by controls on fossil-fuel combustion and industrial production, emissions in this region dropped dramatically between 1970 and 2010. Though these initiatives should continue to be pressed, the gains in terms of additional reductions in atmospheric concentrations are reduced as time goes on because their benefits have been almost fully realized. We thus propose that emphasis needs to shift to Asia, where a similar set of policies to the ones implemented in the North Atlantic region can reduce the emissions growth there and begin to drive down both regional and global emissions. Trends in China in the past decade illustrate that large reductions in Hg emissions can be achieved by targeting coal-fired power plants and other industrial sources. To achieve the greatest declines in Hg concentrations, the North Atlantic model of elimination of intentional Hg use is necessary in Asia and elsewhere. In addition, ASGM, which has slowly driven up emissions in Africa and selected other areas around the world, needs urgent attention. Improved gold extraction techniques that reduce Hg emissions are urgently needed. Focusing on these topical areas within the framework of the Minamata Convention would achieve the greatest benefits.

Acknowledgements

This work was supported by the Electric Power Research Institute under Contract No. 10004163 at Argonne National Laboratory and Contract No. 10005277 at Harvard University. Argonne National Laboratory is operated by UChicago Argonne, LLC, under Contract No. DE-AC02-06CH11357 with the U.S. Department of Energy. We are grateful to Peter Maxson for providing the 2015 data on commercial mercury usage.

References

- Amos, H.M., Jacob, D.J., Kocman, D., Horowitz, H.M., Zhang, Y., Dutkiewicz, S., Horvat, M., Corbitt, E.S., Krabbenhoft, D.P., Sunderland, E.M., 2014. Global biogeochemical implications of mercury discharges from rivers and sediment burial. *Environ. Sci. Technol.* 48, 9514–9522.
- Amos, H.M., Jacob, D.J., Streets, D.G., Sunderland, E.M., 2013. Legacy impacts of all-time anthropogenic emissions on the global mercury cycle. *Global Biogeochem. Cycles* 27, 410–421.
- Amos, H.M., Sonke, J.E., Obrist, D., Robins, N., Hagan, N., Horowitz, H.M., Mason, R.P., Witt, M., Hedgecock, I., Corbitt, E.S., Sunderland, E., 2015. Observational and

modeling constraints on global anthropogenic enrichment of mercury. *Environ. Sci. Technol.* 49, 4036–4047.

- Arctic Monitoring and Assessment Programme (AMAP)/United Nations Environment Programme (UNEP), 2013. Technical Background Report for the Global Mercury Assessment 2013; Oslo. Norway/UNEP Chemicals Branch, Geneva, Switzerland.
- Bagnato, E., Tamburello, G., Avaró, G., Martínez-Cruz, M., Enrico, M., Fu, X., Sprovieri, M., Sonke, J.E., 2014. Mercury fluxes from volcanic and geogenic sources: an update. In: Zellmer, G., Edmonds, M., Straub, S. (Eds.), *Volatiles and Their Role in Petrogenetic and Eruptive Processes at Subduction Zones*, the Geological Society of London Special Publication, vol. 410 The Geological Society of London, London 2014.
- Bond, T.C., Bhardwaj, E., Dong, R., Jogani, R., Jung, S., Roden, C., Streets, D.G., Trautmann, N.M., 2007. Historical emissions of black and organic carbon aerosol from energy-related combustion, 1850–2000. *Global Biogeochem. Cycles* 21, GB2018. <https://doi.org/10.1029/2006GB002840>.
- Bond, T.C., Streets, D.G., Yarber, K.F., Nelson, S.M., Woo, J.-H., Klimont, Z., 2004. A technology-based global inventory of black and organic carbon emissions from combustion. *J. Geophys. Res.* 109, D14203. <https://doi.org/10.1029/2003JD003697>.
- Chakraborty, L.B., Qureshi, A., Vadenbo, C., Hellweg, S., 2013. Anthropogenic mercury flows in India and impacts of emission controls. *Environ. Sci. Technol.* 47, 8105–8113.
- Corbitt, E.S., Jacob, D.J., Holmes, C.D., Streets, D.G., Sunderland, E.M., 2011. Global source-receptor relationships for mercury deposition under present-day and 2050 emissions scenarios. *Environ. Sci. Technol.* 45, 10477–10484.
- De Simone, F., Hedgecock, I.M., Carbone, F., Cinnirella, S., Sprovieri, F., Pirrone, N., 2017. Estimating uncertainty in global mercury emission source and deposition receptor relationships. *Atmosphere* 8, 236. <https://doi.org/10.3390/atmos8120236>.
- Ebinghaus, R., Jennings, S.G., Kock, H.H., Derwent, R.G., Manning, A.J., Spain, T.G., 2011. Decreasing trends in total gaseous mercury observations in baseline air at Mace Head, Ireland from 1996 to 2009. *Atmos. Environ.* 45, 3475–3480.
- Evers, D.C., Keane, S.E., Basu, N., Buck, D., 2016. Evaluating the effectiveness of the Minamata convention on mercury: principles and recommendations for next steps. *Sci. Total Environ.* 569, 888–903.
- Fisher, J.A., Jacob, D.J., Soerensen, A.L., Amos, H.M., Steffen, A., Sunderland, E.M., 2012. Riverine source of Arctic Ocean mercury inferred from atmospheric observations. *Nat. Geosci.* 5, 499–504.
- Fritz, M.M.C., Maxson, P.A., Baumgartner, R.J., 2016. The mercury supply chain, stakeholders and their responsibilities in the quest for mercury-free gold. *Resour. Pol.* 50, 177–192.
- Fu, X.W., Zhang, H., Yu, B., Wang, X., Lin, C.-J., Feng, X.B., 2015. Observations of atmospheric mercury in China: a critical review. *Atmos. Chem. Phys.* 15, 9455–9476.
- Giang, A., Stokes, L.C., Streets, D.G., Corbitt, E.S., Selin, N.E., 2015. Impacts of the Minamata Convention on mercury emissions and global deposition from coal-fired power generation in Asia. *Environ. Sci. Technol.* 49, 5326–5335.
- Gustin, M.S., Evers, D.C., Bank, M.S., Hammerschmidt, C.R., Pierce, A., Basu, N., Blum, J., Bustamante, P., Chen, C., Driscoll, C.T., Horvat, M., Jaffe, D., Pacyna, J., Pirrone, N., Selin, N., 2016. Importance of integration and implementation of emerging and future mercury research into the Minamata Convention. *Environ. Sci. Technol.* 50, 2767–2770.
- Horowitz, H.M., Jacob, D.J., Amos, H.M., Streets, D.G., Sunderland, E.M., 2014. Historical mercury releases from commercial products: global environmental

- implications. *Environ. Sci. Technol.* 48, 10242–10250.
- Horowitz, H.M., Jacob, D.J., Zhang, Y., Dibble, T.S., Slemr, F., Amos, H.M., Schmidt, J.A., Corbitt, E.S., Marais, E.A., Sunderland, E.M., 2017. A new mechanism for atmospheric mercury redox chemistry: implications for the global mercury budget. *Atmos. Chem. Phys.* 17, 6353–6371.
- Huang, Y., Deng, M., Li, T., Japenga, J., Chen, Q., Yang, X., He, Z., 2017. Anthropogenic mercury emissions from 1980 to 2012 in China. *Environ. Pollut.* 226, 230–239.
- International Monetary Fund (IMF), 2018. Gross Domestic Product (Current Prices; Purchasing Power Parity; Billions of International Dollars). [imf-dm-export-20180119.xls](https://data.imf.org/?ts=CountryList).
- Jiskra, M., Sonke, J.E., Obrist, D., Bieser, J., Ebinghaus, R., Myhre, C.L., Pfaffhuber, K.A., Wängberg, I., Kyllönen, K., Worthy, D., Martin, L.G., Labuschagne, C., Mkololo, T., Ramonet, M., Magand, O., Dommergue, A., 2018. A vegetation control on seasonal variations in global atmospheric mercury concentrations. *Nat. Geosci.* 11, 244–250.
- Korsbakken, J.I., Peters, G.P., Andrew, R.M., 2016. Uncertainties around reductions in China's coal use and CO₂ emissions. *Nat. Clim. Change* 6, 687–691.
- Li, C., McLinden, C., Fioletov, V., Krotkov, N., Carn, S., Joiner, J., Streets, D., He, H., Ren, X., Li, Z., Dickerson, R.R., 2017. India is overtaking China as the world's largest emitter of anthropogenic sulfur dioxide. *Sci. Rep.* 7, 14304. <https://doi.org/10.1038/s41598-017-14639-8>.
- Liu, Z., Guan, D., Wei, W., Davis, S.J., Ciais, P., Bai, J., Peng, S., Zhang, Q., Hubacek, K., Marland, G., Andres, R.J., Crawford-Brown, D., Lin, J., Zhao, H., Hong, C., Boden, T.A., Feng, K., Peters, G.P., Xi, F., Liu, J., Li, Y., Zhao, Y., Zeng, N., He, K., 2015. Reduced carbon emission estimates from fossil fuel combustion and cement production in China. *Nature* 524, 335–338.
- Martin, L.G., Labuschagne, C., Brunke, E.-G., Weigelt, A., Ebinghaus, R., Slemr, F., 2017. Trend of atmospheric mercury concentrations at Cape Point for 1995–2004 and since 2007. *Atmos. Chem. Phys.* 17, 2393–2399.
- Muntean, M., Janssens-Maenhout, G., Song, S., Selin, N.E., Olivier, J.G.J., Guizzardi, D., Maas, R., Dentener, F., 2014. Trend analysis from 1970 to 2008 and model evaluation of EDGARv4 global gridded anthropogenic mercury emissions. *Sci. Total Environ.* 494–495, 337–350.
- Muntean, M., Janssens-Maenhout, G., Song, S., Giang, A., Selin, N.E., Zhong, H., Zhao, Y., Olivier, J.G.J., Guizzardi, D., Crippa, M., Schaaf, E., Dentener, F., 2018. Evaluating EDGARv4.tox2 speciated mercury emissions ex-post scenarios and their impacts on modelled global and regional wet deposition patterns. *Atmos. Environ.* 184, 56–68.
- Qiu, J., 2013. Tough talk over mercury treaty. *Nature* 493, 144–145.
- Read, K.A., Neves, L.M., Carpenter, L.J., Lewis, A.C., Fleming, Z.F., Kentisbeer, J., 2017. Four years (2011–2015) of total gaseous mercury measurements from the Cape Verde Atmospheric Observatory. *Atmos. Chem. Phys.* 17, 5393–5406.
- Seccatore, J., Veiga, M., Origiasso, C., Marin, T., De Tomi, G., 2014. An estimation of the artisanal small-scale production of gold in the world. *Sci. Total Environ.* 496, 662–667.
- Selin, N.E., 2018. A proposed global metric to aid mercury pollution policy. *Science* 360, 607–609.
- Sprovieri, F., et al., 2016. Atmospheric mercury concentrations observed at ground-based monitoring sites globally distributed in the framework of the GMOS network. *Atmos. Chem. Phys.* 16, 11915–11935.
- Streets, D.G., Bond, T.C., Lee, T., Jang, C., 2004. On the future of carbonaceous aerosol emissions. *J. Geophys. Res.* 109, D24212. <https://doi.org/10.1029/2004JD004902>.
- Streets, D.G., Devane, M.K., Lu, Z., Bond, T.C., Sunderland, E.M., Jacob, D.J., 2011. All-time releases of mercury to the atmosphere from human activities. *Environ. Sci. Technol.* 45, 10485–10491.
- Streets, D.G., Horowitz, H.M., Jacob, D.J., Lu, Z., Levin, L., ter Schure, A.F.H., Sunderland, E.M., 2017. Total mercury released to the environment by human activities. *Environ. Sci. Technol.* 51, 5969–5977.
- Streets, D.G., Lu, Z., Levin, L., ter Schure, A.F.H., Sunderland, E.M., 2018. Historical releases of mercury to air, land, and water from coal combustion. *Sci. Total Environ.* 615, 131–140.
- Tang, Y., Wang, S., Wu, Q., Liu, K., Wang, L., Li, S., Gao, W., Zhang, L., Zheng, H., Li, Z., Hao, J., 2018. Recent decrease trend of atmospheric mercury concentrations in East China: the influence of anthropogenic emissions. *Atmos. Chem. Phys.* 18, 8279–8291.
- Telmer, K., Viega, M., 2008. World emissions of mercury from artisanal and small scale gold mining. In: Pirrone, N., Mason, R. (Eds.), *Interim Report of the UNEP Global Partnership on Atmospheric Mercury Transport and Fate Research*.
- United Nations, 2017. World Population Data. [POP/DB/WPP/Rev.2017/POP/F01-1](https://data.un.org/Data.aspx?ds=POP&dsq=POP/DB/WPP/Rev.2017/POP/F01-1).
- United Nations Environment Programme (UNEP), 2013. *United Nations Environment Programme (UNEP). Global Mercury Assessment 2013: Sources, Emissions, Releases and Environmental Transport*, Geneva, Switzerland.
- United Nations Environment Programme (UNEP), 2017. *Global Mercury Supply, Trade and Demand*. (Geneva, Switzerland).
- Veiga, M.M., Angeloci-Santos, G., Meech, J.A., 2014. Review of barriers to reduce mercury use in artisanal gold mining. *Extr. Ind. Soc.* 1, 351–361.
- Weigelt, A., Ebinghaus, R., Manning, A.J., Derwent, R.G., Simmonds, P.G., Spain, T.G., Jennings, S.G., Slemr, F., 2015. Analysis and interpretation of 18 years of mercury observations since 1996 at Mace Head, Ireland. *Atmos. Environ.* 100, 85–93.
- Weiss-Penzias, P.S., Gay, D.A., Brigham, M.E., Parsons, M.T., Gustin, M.S., ter Schure, A., 2016. Trends in mercury wet deposition and mercury air concentrations across the US and Canada. *Sci. Total Environ.* 568, 546–556.
- World Bank, 2018. *World development indicators, industrial value added (current US\$)*. <https://data.worldbank.org/indicator/NV.IND.TOTL.CD>.
- Wu, Q.R., Wang, S.X., Zhang, L., Song, J.X., Yang, H., Meng, Y., 2012. Update of mercury emissions from China's primary zinc, lead and copper smelters, 2000–2010. *Atmos. Chem. Phys.* 12, 11153–11163.
- Wu, Y., Streets, D.G., Wang, S.X., Hao, J.M., 2010. Uncertainties in estimating mercury emissions from coal-fired power plants in China. *Atmos. Chem. Phys.* 10, 2937–2947.
- Xu, Y., Williams, R.H., Socolow, R.H., 2009. China's rapid deployment of SO₂ scrubbers. *Energy Environ. Sci.* 2, 459–465.
- Zhang, L., Wang, S., Wang, L., Wu, Y., Duan, L., Wu, Q., Wang, F., Yang, M., Yang, H., Hao, J., Liu, X., 2015. Updated emission inventories for speciated atmospheric mercury from anthropogenic sources in China. *Environ. Sci. Technol.* 49, 3185–3194.
- Zhang, Y., Jacob, D.J., Horowitz, H.M., Chen, L., Amos, H.M., Krabbenhoft, D.P., Slemr, F., St Louis, V.L., Sunderland, E.M., 2016. Observed decrease in atmospheric mercury explained by global decline in anthropogenic emissions. *Proc. Natl. Acad. Sci. USA* 113, 526–531.